Thermal modification of in-medium mesons from screening properties on the lattice

Yu Maezawa[*]

Fakultät für Physik, Universität Bielefeld, D-33615 Bielefeld, Germany
E-mail: ymaezawa@physik.uni-bielefeld.de

Alexei Bazavov

Department of Physics and Astronomy, University of Iowa, Iowa City, Iowa 52240, USA

Frithjof Karsch

Physics Department, Brookhaven National Laboratory, Upton, NY 11973, USA
Fakultät für Physik, Universität Bielefeld, D-33615 Bielefeld, Germany

Peter Petreczky

Physics Department, Brookhaven National Laboratory, Upton, NY 11973, USA

Swagato Mukherjee

Physics Department, Brookhaven National Laboratory, Upton, NY 11973, USA

Screening and melting properties of the mesonic excitations are studied from spatial correlation functions in (2+1)-flavor lattice QCD simulations with the highly improved staggered quark action. A comparative study of the in-medium modifications of mesons consisting strange–anti-strange, strange–anti-charm and charm–anti-charm quarks is performed. We observe significant in-medium modifications for the ϕ and D_s meson channels already at temperatures around the chiral crossover region. On the other hand, for the J/ψ and η_c meson channels in-medium modifications remain relatively small around the chiral crossover region and become significant only above 1.3 times the chiral crossover temperature.

9th International Workshop on Critical Point and Onset of Deconfinement
17-21 November, 2014
ZiF (Center of Interdisciplinary Research), University of Bielefeld, Germany

---

[*]Speaker.

1. Introduction

At high temperatures matter controlled by the strong force undergoes a chiral crossover transition [1], accompanied by the deconfinement of flavor quantum numbers carrying degrees of freedom [2]. The relevant degrees of freedom change from hadrons to quarks and gluons (see *e.g.* Refs. [3, 4] for recent reviews). The in-medium modification and dissolution of heavy quarkonium were suggested as a signal for creating a deconfined medium in heavy ion collisions by Matsui and Satz [5]. The existence of heavy-light mesons above the chiral transition temperature has also been proposed to explain the large energy loss and flow of heavy quarks observed in heavy ion collisions [6]. Recent lattice QCD calculations suggest that heavy-light bound states dissolve already at or close to the QCD transition temperature based on flavor and quantum number correlation analysis [7].

Hadronic correlation functions have long been advocated as convenient tools to explore the properties of strong interaction matter [8]. They encode the in-medium properties of hadrons, as well as their dissolution. Moreover, through the comparison of lattice results with weak coupling calculations at high temperature [9, 10] they also provide information on the change from strongly to weakly interacting matter.

Spectral functions, the Fourier transforms of real time meson correlation function, are the basic quantities that provide knowledge regarding the in-medium properties of mesons and their dissolution. Meson states appear as peaks in the corresponding spectral functions with the peak position equal to the meson mass. The width of the peak corresponds to the in-medium width of the meson. However, lattice QCD is formulated in Euclidean space time. Temporal meson correlation functions calculated on the lattice,

$$G(\tau, \vec{p}, T) = \int d^3x e^{i\vec{p}\cdot\vec{x}} \langle J_H(\tau, \vec{x}) J_H(0, \vec{0}) \rangle , \qquad (1.1)$$

have a simple relation to the spectral function, $\sigma(\omega, \vec{p}, T)$:

$$G(\tau, \vec{p}, T) = \int_0^\infty d\omega \sigma(\omega, \vec{p}, T) K(\omega, \tau, T), \quad K(\omega, \tau, T) = \frac{\cosh(\omega(\tau - 1/2T))}{\sinh(\omega/2T)}. \qquad (1.2)$$

Here J_H is a meson operator, typically of the form $J_H = \bar{q}\Gamma_H q$, with Γ_H being some combination of the Dirac matrices that specifies the quantum numbers of the meson. One way to obtain the spectral function from the above relation is to use the maximum entropy method [11, 12, 13, 14, 15]. The analysis of temporal correlation functions is difficult due to the limited extent, $1/T$, in Euclidean time direction. In the case of heavy quarkonium correlators, for instance, it turned out that the melting of bound states does not lead to large changes in the correlation functions [15]. In order to become sensitive to the corresponding disappearance of a resonance peak in the spectral function high statistical accuracy and the analysis of the correlation function at a large number of Euclidean time separations are needed. At fixed temperature $T = 1/N_\tau a$, this requires large lattices with temporal extent N_τ and sufficiently small lattice spacing, a.

Alternatively, one can study the spatial correlation functions of mesons

$$G(z, T) = \int_0^{1/T} d\tau \int dx dy \langle J_H(\tau, x, y, z) J_H(0, 0, 0, 0) \rangle. \qquad (1.3)$$

These are related to the spectral functions in a more complicated way that also involves integration of momenta,

$$G(z,T) = \int_0^\infty \frac{2d\omega}{\omega} \int_{-\infty}^\infty dp_z e^{ip_z z} \sigma(\omega, p_z, T).$$ (1.4)

Since the spatial separation is not limited by the inverse temperature, the spatial correlation function can be studied at separations larger than $1/T$. Therefore, the spatial correlation functions can be more sensitive to in-medium modifications and/or the dissolution of mesons. Another advantage of spatial correlation functions over the temporal ones is that the spatial correlation function can be directly compared to the corresponding vacuum correlation function to quantify modifications of the in-medium spectral function. It is apparent from Eq. (1.2) that for the temporal correlation function the temperature dependent in-medium modifications of the spectral function are partly masked by the temperature dependence of the Kernel $K(\omega, \tau, T)$, and a comparison with the corresponding vacuum correlation function demands evaluation of the reconstructed correlator [13]. Such complication is not present for the spatial correlation functions.

While the general relation between spectral functions and spatial meson correlators is more involved, in some limiting cases it becomes simple. At large distances the spatial correlation functions decay exponentially, $G(z,T) \sim \exp(-M(T)z)$, where M is known as the *screening mass*. Note that, unlike the in-medium temporal correlation functions, the transport contributions to the spectral functions at small frequencies do not lead to a non-decaying constant in the large distance behavior of the spatial correlation functions. At small enough temperatures when there exists a well-defined mesonic bound state, the spectral function has the form $\sigma(\omega, 0, 0, p_z, T) \sim \delta(\omega^2 - p_z^2 - m_0^2)$, and M becomes equal to the (pole) mass m_0 of the meson. On the other hand, at high enough temperatures, when the mesonic excitations are completely melted, the spatial meson correlation functions describe the propagation of a free quark-antiquark pair. The screening masses are then given by $M_{\text{free}} = 2\sqrt{m^2 + (\pi T)^2}$ where m is the masses of the quark and anti-quark that form the meson [16]. This form of the screening mass in the non-interacting limit is a direct consequence of the anti-periodic boundary conditions in Euclidean time that are needed for the representation of fermions at non-zero temperature. This leads to the appearance of a smallest non-zero Matsubara frequency, πT, in the quark and anti-quark propagators. As the bosonic meson state is dissolved in the non-interacting limit the screening mass results as the contribution of two independently propagating fermionic degrees of freedom. Thus the transition between these two limiting values of the screening mass can be used as an indicator for the thermal modification and eventual dissolution of mesonic excitations.

Lattice QCD studies of the screening masses of light quark mesons have been performed within the quenched approximation [17] and also with two dynamical flavors using staggered [18] as well as Wilson-type quarks [19]. Screening masses in the light and strange quark sector have been studied recently in $(2+1)$-flavor QCD using the so-called p4 staggered fermion action [20] and the expected qualitative behavior discussed above was observed. Furthermore, the study has been extended to the case of charmonium providing the first direct evidence for melting of the charmonium ground state [21] from lattice QCD with light dynamical quark degrees of freedom.

In this work we report on studies of spatial meson correlators and screening masses using the Highly Improved Staggered Quark (HISQ) action [22] with a strange quark mass tuned to its physical value and almost physical, degenerate up and down quark masses. The HISQ action is

known to lead to discretization effects that are smaller than those observed with all other staggered-type actions currently used in studies of lattice QCD thermodynamics [23]. Moreover, the HISQ action is well suited to study heavy quarks on the lattice [22] and turned out to be successful in quantitative studies of charmonium and *D* meson properties [24]. In this work we study the spatial correlation functions of mesonic excitations with strange (*s*) and charm (*c*) quarks, specifically the lowest states in the pseudo-scalar, vector, scalar and axial-vector channels for the $s\bar{s}$, $s\bar{c}$ and $c\bar{c}$ flavor combinations. This study has been summarized in Ref. [25]

2. Lattice setup

We calculate meson correlation functions on gauge configurations generated in $(2+1)$-flavor QCD using the HISQ action [23]. The strange quark mass m_s is adjusted to its physical value and the light quark masses are fixed at $m_l = m_s/20$, corresponding to $m_\pi \simeq 160$ MeV and $m_K \simeq 504$ MeV at zero temperature in the continuum limit [23]. Charm quarks are introduced as valance quarks and we use the HISQ action with the so-called ε-term for the charm quark mass [22] which makes our calculations in the heavy quark sector free of tree-level discretization errors up to $\mathscr{O}((am_c)^4)$. The charm quark mass is also determined to reproduce the spin-averaged charmonium mass, $(m_{\eta_c} + 3m_{J/\psi})/4$ [25]. Our calculations have been performed on lattices of size $N_\sigma^3 \times N_\tau = 48^3 \times 12$. We consider lattice couplings in the range $\beta =$ 6.664–7.280 which correspond to temperatures $T =$ 138–248 MeV. This enables investigation of in-medium modifications of meson properties below and above the chiral crossover transition at $T_c = (154 \pm 9)$ MeV [23]. To study the spatial correlators at higher temperatures we adopt the fixed-scale approach and perform calculations at $\beta = 7.280$ for $N_\tau = 10, 8, 6, 4$ which corresponds to the temperature range $T =$ 298–744 MeV. In all our calculations the spatial extent of the lattice is four times the temporal extent: $N_\sigma = 4N_\tau$. The lattice spacing and the resulting temperature values, $T = 1/N_\tau a$, have been determined using results for the kaon decay constant [23].

In the staggered formulation a quark contains four valence tastes and meson operators are defined as $J_H = \bar{q}(\Gamma^D \times \Gamma^F)q$, Γ^D and Γ^F being products of the Dirac Gamma matrices which generate spin and taste structures, respectively [26]. In this study, we focus only on local meson operators with $\Gamma^D = \Gamma^F = \Gamma$. By using staggered quark fields $\chi(\boldsymbol{x})$ at $\boldsymbol{x} = (x, y, z, \tau)$ the meson operators can be written as $J_H(\boldsymbol{x}) = \tilde{\phi}(\boldsymbol{x})\bar{\chi}(\boldsymbol{x})\chi(\boldsymbol{x})$, where $\tilde{\phi}(\boldsymbol{x})$ is a phase factor depending on the choice of Γ. We calculate only the quark-line connected part of the meson correlators since the effect due to the disconnected part is expected to be small. The spatial correlation function along the *z* direction is defined as the meson propagator projected to zero transverse momentum. Since a staggered meson correlator contains two different mesons with opposite parities, at large distances the lattice correlator can be parametrized as

$$G(z) = A_{NO}^2 \left(e^{-M_- z} + e^{-M_- (N_z - z)} \right) - (-1)^z A_O^2 \left(e^{-M_+ z} + e^{-M_+ (N_z - z)} \right) \qquad (2.1)$$

where the first (second) term in the right-hand-side characterizes a non-oscillating (oscillating) contribution governed by a negative (positive) parity state. Since at non-zero temperatures the rotational symmetry of the spatial correlations functions reduces to $O(2) \times Z(2)$, the vector meson states must be decomposed into transverse and longitudinal components. Here we focus on the meson screening masses in the pseudo-scalar ($J^P = 0^-$), scalar (0^+), vector-transverse (1^-) and axial-vector-transverse (1^+) channels. Corresponding Γ and $\tilde{\phi}(\boldsymbol{x})$ are summarized in Ref. [25]. At zero
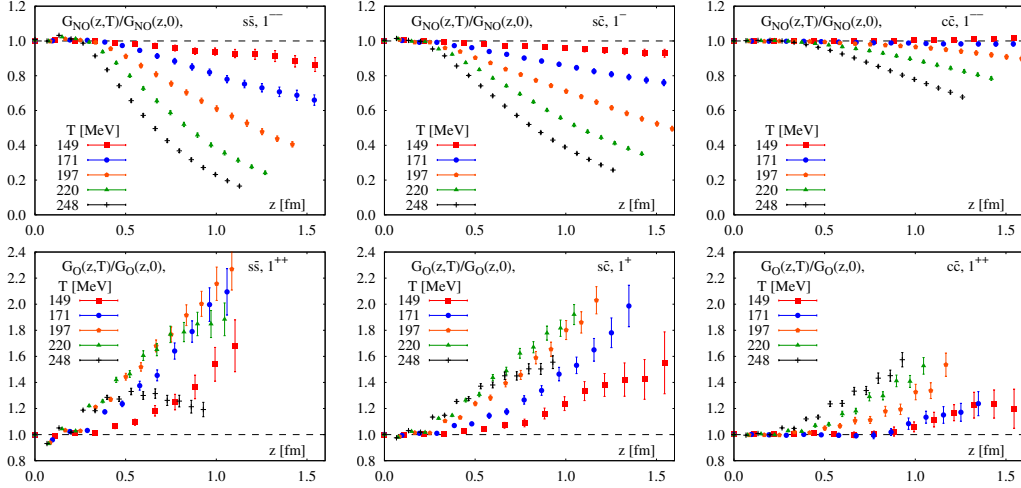
Figure 1: Ratios of the non-oscillating (negative parity) part of vector correlators (top) and the oscillating (positive parity) part of axial-vector correlators (bottom) in $s\bar{s}$ (left), $s\bar{c}$ (middle) and $c\bar{c}$ (right) sectors at different temperatures to the corresponding zero temperature results.

temperature, these correspond to $(0^-, 0^+, 1^-, 1^+) = (\eta_{s\bar{s}}, -, \phi, f_1(1420))$, $(D_s, D_{s0}^*, D_s^*, D_{s1})$ and $(\eta_c, \chi_{c0}, J/\psi, \chi_{c1})$, respectively, where $\eta_{\bar{s}s}$ is an unphysical state with the mass $M_{\eta_{\bar{s}s}} = \sqrt{2M_K^2 - M_\pi^2}$.

3. Temperature dependence of spatial meson correlators

We start the discussion of our results with the temperature dependence of meson correlators. It was pointed out in Ref. [21], contrary to the temporal correlation functions, spatial correlation functions show visible changes already in the vicinity of the crossover temperature even in the case of charmonium. Since staggered meson correlators in each channel contain both negative parity (non-oscillating) and positive parity (oscillating) states, it is important to separate these contributions before studying the temperature dependence of the correlators. As discussed in detail in Ref. [25], it is possible to define two separate effective correlators for the negative (non-oscillating, *NO*) and positive (oscillating, *O*) parity states of a staggered meson correlation function $G(z)$

$$G_{NO}(z) \equiv A_{NO}^2(z) e^{-M_-(z)z} = \frac{g_1 + g_0 x_+}{x_- + x_+}, \quad G_O(z) \equiv A_O^2(z) e^{-M_+(z)z} = (-1)^z \frac{g_1 - g_0 x_-}{x_- + x_+},$$

in terms of the local, effective masses, $x_\pm(z) = e^{-M_\pm(z)}$, obtained by solving the equations, $Ax_\pm^2 \mp Bx_\pm + C = 0$ with $A = g_1^2 - g_2 g_0$, $B = g_3 g_0 - g_2 g_1$, $C = g_2^2 - g_3 g_1$, and $g_i \equiv G(z+i), i = 0,1,2,3$ being the values of the meson correlation function at four successive z values. In this description we neglect contribution of periodic boundary to the propagating direction. Further, one can form ratios of these contributions at different temperatures to the corresponding zero temperature results. As discussed before, in contrast to temporal correlation functions, such ratio can directly probe the thermal modifications of the spectral functions themselves. If there is no change in the meson spectral functions, these ratios will be equal to one and deviations from unity will indicate in-medium modification of the meson spectral functions at non-zero temperature.

In Fig. 1 (top), we show the ratio of the negative parity part of the vector correlator in $s\bar{s}$, $s\bar{c}$ and $c\bar{c}$ channels to the corresponding zero temperature correlator, obtained with point sources. At

zero temperature, these non-oscillating parts of vector correlators are dominated by ϕ, D_s^* and J/ψ states, respectively. In the $s\bar{s}$ sector, at large distances, we observe $\sim 18\%$ and $\sim 38\%$ decrease of this ratio at $T = 149$ MeV and 171 MeV, respectively. A somewhat smaller but still significant, $\sim 8\%$ and $\sim 20\%$ respectively, decrease of this ratio is also seen in the $s\bar{c}$ sector. Note that, recent lattice studies based on flavor and quantum number correlations [2, 7] have strongly suggested that open strange and charm mesons start to melt already around $T_c = (154 \pm 9)$ MeV. Thus, a $\sim 20\%$ deviation of the in-medium correlator with respect to the vacuum one depicts a thermally modified spectral function with melted meson state. For ratios in the J/ψ sector no changes are visible at the lowest 149 MeV temperature, and even at $T = 171$ MeV the deviations of this ratio from unity are at best a few percent. For charmonia the deviations of the in-medium correlators, at large distances, with respect to the vacuum ones become larger than 20% only for $T \gtrsim 200$ MeV. In all cases, the ratio of correlators decreases with increasing temperature at large distances. As we will see in the next section this is related to the fact that screening masses in the negative parity channels increase with respect to their vacuum values with increasing temperature.

In Fig. 1 (bottom), we show the ratio of the positive parity (oscillating) part of the axial-vector correlator in $s\bar{s}$, $s\bar{c}$ and $c\bar{c}$ channels to the corresponding zero temperature correlator, again obtained with point sources. The meson states that dominate the oscillating part of these correlators are $f_1(1420)$, D_{s1} and χ_{c1}. The ratios of the correlators in this case show a more complex behavior. At relatively short distance the ratios of the correlators increases, then depending on the temperature value and the quark content the ratio can also decrease both as function of z and the temperature. As will be discussed in the next section, this feature of the correlator ratios is closely related to the behavior of screening masses of the positive parity states. For not too large temperatures the positive parity screening masses decrease compared to their vacuum values. This corresponds to the increase in the ratio of the correlators at large z. At sufficiently high temperature the screening masses start to increase again, which then leads to the decrease in the ratio of the positive parity correlators. This tendency is seen in the $s\bar{s}$ and $s\bar{c}$ sectors in Fig. 1 (bottom).

The ratio of spatial charmonium correlators and corresponding zero temperature correlators were first studied in Ref. [21] in the pseudo-scalar channel. Strong in-medium modifications of this ratio was found for $zT > 1$. The magnitude of medium effects in the ratios of pseudo-scalar correlators calculated with the HISQ action is similar to those obtained previously with the p4 action at the same value of T/T_c. The large changes in the ratio of the spatial correlators, that could be indicative of significant in-medium modification or dissolution of $1S$ charmonium states, are in contrast to the very mild temperature dependence of the analogous ratios of the reconstructed temporal correlators. The reason for this apparent difference lies in the fact that at non-zero temperature the temporal correlators are defined only at relatively small separations $\tau < 1/(2T)$ and, thus have a limited sensitivity to the in-medium modifications of the spectral functions. As one can see from Fig. 1 the medium modification of the spatial correlators for $z < 1/(2T)$ is also quite small. As discussed in the section I the access to larger separation is the main reason why the spatial correlation functions are more sensitive to the in-medium modification of the spectral functions.

4. Large distance behavior of spatial meson correlators and screening masses

We fit the large distance behavior of the spatial correlators using Eq. (2.1) and extract screening
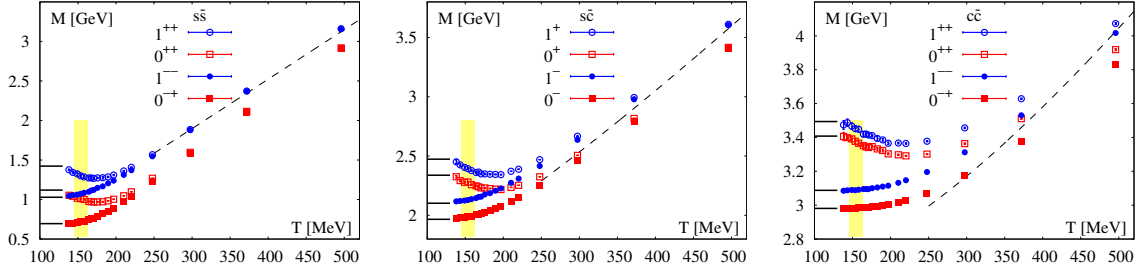
Figure 2: Screening masses for different channels in $s\bar{s}$ (top), $s\bar{c}$ (middle) and $c\bar{c}$ (bottom) sectors as functions of the temperature. The solid horizontal lines on the left depict the corresponding zero temperature meson masses. The shaded regions indicate the chiral crossover temperature $T_c = (154 \pm 9)$ MeV. The dashed lines are the corresponding free field theory result (see text).

masses in various channels for $s\bar{s}$, $s\bar{c}$ and $c\bar{c}$ mesons. All our results on screening masses in the $s\bar{s}$, $s\bar{c}$ and $c\bar{c}$ sectors are shown in Fig. 2. We expect that at very high temperature the screening masses are given by M_{free}. We show the free theory (leading order perturbative) results as dashed lines in Fig. 2, where the charm quark mass is decided as the renormalization scale $m_c(\bar{\mu} = m_c) = 1.275$ GeV from Particle Data Group [27] and the strange quark mass is estimated from the renormalization invariant ratio $m_c/m_s = 11.85$ [28] with the above m_c. This completely specifies our free theory prediction.

As one can see from Fig. 2, there are three distinct regions: the low temperature region, where the screening masses are close to the corresponding vacuum masses (solid lines), the intermediate temperature region, where we see significant changes in the value of the screening masses with respect to the corresponding vacuum masses, and finally, the high temperature region, where the screening masses are close to the free theory result (dashed lines). In the high temperature region, there clearly are no meson bound states anymore. The onset of the high temperature behavior is different in different sectors. In the $s\bar{s}$ sector it starts at around $T = 210$ MeV. In the $s\bar{c}$ sector it starts at $T = 250$ MeV, while in $c\bar{c}$ sector it starts at $T > 300$ MeV. As the temperature increases, we see that the screening masses corresponding to negative parity states increase monotonically, while the screening masses in the positive parity states first decrease before starting to rise towards the asymptotic high temperature values. In the intermediate temperature region the screening masses of opposite parity partners start to approach each other and we observe a significant rearrangement of the ordering of screening masses in different channels. At sufficiently high temperatures the pseudo-scalar and scalar (0^{-+} and 0^{++}) as well as vector and axial-vector (1^{--} and 1^{++}) screening masses become degenerate. In the $s\bar{s}$ sector this is evident for $T > 220$ MeV, while for the two other sectors it happens at higher temperatures due to the larger explicit breaking of parity by the charm quark mass. In the high temperature region the screening masses in the pseudo-scalar channel are smaller than the screening masses in the vector channel.

In order to emphasize the different behavior of negative and positive parity screening masses in the low and intermediate temperature regions it is convenient to consider the difference between the screening mass and the corresponding vacuum masses m_0 calculated at $T = 0$: $\Delta M(T) = M(T) - m_0$. It is tempting to interpret this difference as the change in the binding energy of meson states, however, the relation between the screening mass and the pole mass only holds as long as there is a well defined bound state. Nonetheless, ΔM could provide some constraints on the change
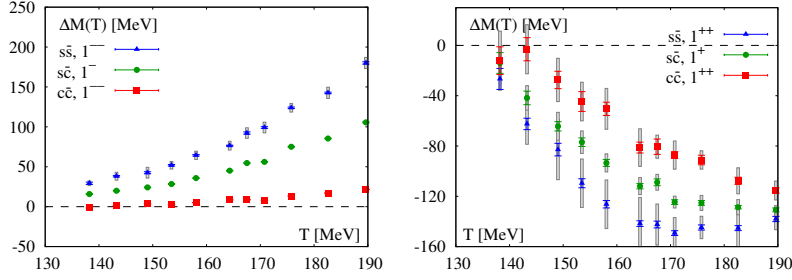
7

Figure 3: The difference, $\Delta M(T) = M(T) - m_0$, of the screening masses, $M(T)$, and the corresponding vacuum masses, m_0, for the negative (left) and positive (right) parity states as functions of the temperature.

of the binding energy in the low and intermediate temperature regions. We show our results for $\Delta M(T)$ for vector (1^-) and axial-vector (1^+) $s\bar{s}$, $s\bar{c}$ and $c\bar{c}$ mesons in Fig. 3. The error bars and gray bands indicate the statistical and systematic errors, respectively. In all cases ΔM increases for negative parity states and decreases for positive parity states in the considered temperature region. This corresponds, of course, directly to the pattern seen in the behavior of ratios of spatial correlation functions (see Fig. 1). At higher temperature the positive parity screening masses will start increasing again (see Fig. 2) leading to the non-monotonic behavior of the correlator ratios in the $s\bar{s}$ and $s\bar{c}$ sectors. Except for the negative parity (S-wave) charmonium states we clearly see that in all other cases in-medium modifications lead to significant deviations of screening masses from pole masses already in the crossover region. In the case of $s\bar{s}$ states this is the case even below T_c. For the S-wave charmonium states screening and pole masses are nearly compatible up to temperatures of about 200 MeV. This is consistent with the small deviations from unity observed for ratios of zero and finite temperature correlators in these quantum number channels and may indicate that these states do persist as bound states at least up to this value of the temperature. Thus, in the charmonium case the temperature dependence of ΔM provides some hints for sequential thermal modification: It shows a strong decrease of screening masses starting in the crossover region for scalar and axial-vector channels corresponding to 1P charmonium states (χ_{c0} and χ_{c1}) and very little change in the pseudo-scalar and vector channels corresponding to 1S charmonium states (η_c and J/ψ).

5. Conclusions

We have studied spatial correlation functions at non-zero temperature for $s\bar{s}$, $s\bar{c}$ and $c\bar{c}$ mesons to investigate their in-medium modifications. We have performed direct comparisons of the in-medium correlation functions with the corresponding zero temperature ones, extracted screening masses from large distance behaviors of the correlation functions. We have found that medium modifications of the spatial meson correlation functions set in the crossover region. However we have also found that the amount of in-medium modifications in the spatial correlators is different in different sectors and decreases with the heavy quark content. The $s\bar{s}$ and $s\bar{c}$ mesons are significantly effected by the medium already at relatively low temperatures and possibly dissolve at temperature close to the crossover temperature, $T_c = (154 \pm 9)$ MeV. For the $c\bar{c}$ mesons, S-wave charmonium states (J/ψ and η_c) undergo very small medium modifications up to $T \sim 1.1 T_c$ ($T \sim 170$ MeV) and significant medium modifications are observed only for $T \gtrsim 1.3 T_c$ ($T \gtrsim 200$ MeV). We have

also seen a clear difference between the temperature dependence of the correlators corresponding to S-wave charmonium and to P-wave charmonium (χ_{c0} and χ_{c1}) states. The spatial correlators corresponding to χ_{c0} and χ_{c1} states show sizable medium modifications already in the crossover region. This is in line with the sequential melting of charmonia states— the larger, loosely bound P-wave states dissociate at lower temperatures than the smaller, tightly bound S-wave charmonia.

Let us finally summurize the importance of our findings for the physics of heavy ion collisions. The sequential charmonium melting is an essential ingredient for most of phenomenological models that attempt to explain charmonium yield in heavy ion collisions. Therefore our findings provide support for these models. The fact that open-charm mesons dissolve at temperatures close to the transition temperature disfavors the models which try to explain the large energy loss of heavy quarks in heavy ion collisions through the existence of heavy-light bound states in quark gluon plasma [6]. Finally the large medium modification of hidden strange meson correlators disfavors scenarios of separate freeze-out of strange degrees of freedom in heavy ion collisions [29].

References

[1] T Bhattacharya, M. I. Buchoff, et al. QCD Phase Transition with Chiral Quarks and Physical Quark Masses. *Phys.Rev.Lett.*, 113(8):082001, 2014.

[2] A. Bazavov, H. T. Ding, et al. Strangeness at high temperatures: from hadrons to quarks. *Phys.Rev.Lett.*, 111:082301, 2013.

[3] P. Petreczky. Lattice QCD at non-zero temperature. *J. Phys.*, G39:093002, 2012.

[4] Owe Philipsen. The QCD equation of state from the lattice. *Prog. Part. Nucl. Phys.*, 70:55, 2013.

[5] T. Matsui and H. Satz. J/ψ Suppression by Quark-Gluon Plasma Formation. *Phys. Lett.*, B178:416, 1986.

[6] R. Sharma, I. Vitev, and B.-W. Zhang. Light-cone wave function approach to open heavy flavor dynamics in QCD matter. *Phys. Rev.*, C80:054902, 2009.

[7] A. Bazavov, H.-T. Ding, et al. The melting and abundance of open charm hadrons. *Phys.Lett.*, B737:210, 2014.

[8] Carleton E. Detar and John B. Kogut. The Hadronic Spectrum of the Quark Plasma. *Phys. Rev. Lett.*, 59:399, 1987.

[9] M. Laine and M. Vepsalainen. Mesonic correlation lengths in high temperature QCD. *JHEP*, 0402:004, 2004.

[10] B.B. Brandt, A. Francis, M. Laine, and H.B. Meyer. A relation between screening masses and real-time rates. *JHEP*, 1405:117, 2014.

[11] I. Wetzorke, F. Karsch, et al. Meson spectral functions at finite temperature. *Nucl. Phys. Proc. Suppl.*, 106:510, 2002.

[12] M. Asakawa and T. Hatsuda. J/psi and eta/c in the deconfined plasma from lattice qcd. *Phys. Rev. Lett.*, 92:012001, 2004.

[13] Saumen Datta, Frithjof Karsch, Peter Petreczky, and Ines Wetzorke. Behavior of charmonium systems after deconfinement. *Phys. Rev.*, D69:094507, 2004.

[14] Gert Aarts, Chris Allton, Mehmet Bugrahan Oktay, Mike Peardon, and Jon-Ivar Skullerud. Charmonium at high temperature in two-flavor QCD. *Phys. Rev.*, D76:094513, 2007.

[15] H.T. Ding, A. Francis, O. Kaczmarek, F. Karsch, H. Satz, et al. Charmonium properties in hot quenched lattice QCD. *Phys. Rev.*, D86:014509, 2012.

[16] W. Florkowski and B. L. Friman. Spatial dependence of the finite temperature meson correlation function. *Z.Phys.*, A347:271, 1994.

[17] R.V. Gavai, Sourendu Gupta, and R. Lacaze. Screening correlators with chiral Fermions. *Phys.Rev.*, D78:014502, 2008.

[18] Debasish Banerjee, Rajiv V. Gavai, and Sourendu Gupta. Quasi-static probes of the QCD plasma. *Phys.Rev.*, D83:074510, 2011.

[19] Hideaki Iida, Yu Maezawa, and Koichi Yazaki. Hadron properties at finite temperature and density with two-flavor Wilson fermions. *PoS*, LATTICE2010:189, 2010.

[20] M. Cheng, S. Datta, A. Francis, J. van der Heide, C. Jung, et al. Meson screening masses from lattice QCD with two light and the strange quark. *Eur. Phys. J.*, C71:1564, 2011.

[21] F. Karsch, E. Laermann, Swagato Mukherjee, and P. Petreczky. Signatures of charmonium modification in spatial correlation functions. *Phys. Rev.*, D85:114501, 2012.

[22] E. Follana et al. Highly improved staggered quarks on the lattice, with applications to charm physics. *Phys. Rev.*, D75:054502, 2007.

[23] A. Bazavov, T. Bhattacharya, M. Cheng, C. DeTar, H.T. Ding, et al. The chiral and deconfinement aspects of the QCD transition. *Phys. Rev.*, D85:054503, 2012.

[24] A. Bazavov et al. Charmed and strange pseudoscalar meson decay constants from HISQ simulations. 2013.

[25] Alexei Bazavov, Frithjof Karsch, Yu Maezawa, Swagato Mukherjee, and Peter Petreczky. In-medium modifications of open and hidden strange-charm mesons from spatial correlation functions. *Phys.Rev.*, D91(5):054503, 2015.

[26] R. Altmeyer et al. The Hadron spectrum in QCD with dynamical staggered fermions. *Nucl. Phys.*, B389:445, 1993.

[27] J. Beringer et al. Review of Particle Physics (RPP). *Phys. Rev.*, D86:010001, 2012.

[28] C.T.H. Davies, C. McNeile, K.Y. Wong, E. Follana, R. Horgan, et al. Precise Charm to Strange Mass Ratio and Light Quark Masses from Full Lattice QCD. *Phys. Rev. Lett.*, 104:132003, 2010.

[29] S. Chatterjee, R.M. Godbole, and Sourendu Gupta. Strange freezeout. *Phys.Lett.*, B727:554, 2013.